Interactive comment on "Virtual full-scale testing for investigating strength characteristics of a composite wind turbine blade" by Can Muyan and Demirkan Coker

Xiao Chen (Referee)
xiac@dtu.dk
Received and published: 9 April 2020

We thank the Referee for the detailed and insightful comments regarding the paper. In our response, we have carried out new simulations in light of his comments where necessary and have added new figures that correct and clarify our work. The comments are individually addressed below, with the Referee's comments written in red and our response in black. If accepted, our response to the Referee's comments will be incorporated in the revised version of the paper which we believe will result in a clearer and more thorough paper.

Comment 1: In essence, this work presented FE simulations of a 5-m full-scale blade subject to static loads using nonlinear puck failure criterion. Instead of using 'virtual full-scale testing', it is more suitable to use 'FE simulations' to reflect the essence of this work. To the reviewer, 'virtual testing' is more than FE simulations.

Response to Comment 1 :
We agree with the referee and we propose to change the title to:
"FE simulations to investigate the strength characteristics of a 5-m composite wind turbine blade"
where we also limited the scope to the existing 5-m blade that we are investigating.

Comment 2: In the abstract, 'so that the physical basis of the progressive damage development can be captured and interpreted correctly.' should change to 'so that the physical basis of the progressive damage development can be better interpreted and understood'. Physical tests capture real damages while FE simulations hopefully can complement experimental observations to achieve better understanding. You may consider to read https://doi.org/10.1016/j.compstruct.2019 .03.018.

Response to Comment 2 :
We agree with the Referee and the abstract is changed according to the comment. In addition, wording used in the abstract and other parts of the paper is replaced with a more precise wording to accurately reflect what we mean.

Comment 3: The big blades behave/fail differently from the smaller ones. Two studies listed below shows that the governing failure mechanisms are quite different. How the results from this study using a 5-m blade FE model are relevant to the blades which are usually more than 10 times longer? Please comment on this.
https://doi.org/10.1007/s11431-014-5741-8 and https://doi.org/10.3390/en7042274

Response to Comment 3:
Chen, Wei Zhao, Lu Zhao and Xu (2014) conducted a full-scale bending test of a 52.3 m wind turbine blade and found that delamination in the spar cap and shear web failure at the root transition region were the main failure mechanisms for the blade collapse. Local buckling contributed to the main failure mechanism by facilitating local out-of-plane deformation. They conclude that for large blades, through-the-thickness stresses which cause debonding and delamination at the blade root transition region need to be considered in the FEA. Chen, Qin, Yang, Zhao and Xu (2015) focused on the local buckling resistance of 10.3 m wind turbine blades. FE analysis showed that configurations with sharp edges are susceptible to local buckling. During testing of the 10.3 m blade, although local buckling of shear web and flatback airfoil was observed, composite laminate failure in these locations was not observed. These results indicate different mechanisms for different blade sizes.

Within the framework of the current study, strength of an existing 5m blade is studied in terms of composite material failure. Further, in response to Referee's comment 10, a linear buckling analysis is conducted. The 5m blade is found to exhibit sufficient resistance against buckling in our investigation (see response to comment 10). However, our current model using Puck's damage model indicates that laminate failure plays a major role for the ultimate blade failure. Our analysis results suggest that debonding and delamination analysis can be useful to properly interpret the results. In addition to damage in the trailing edge, we found that the thin and stiff internal flange located at the leading edge is damaged primarily under flap-wise loading condition for the 5m blade. The simulation results will be compared with experiments to be conducted at RUZGEM on a 5 m blade which will be a follow-up to this study.

Comment 4: In Chen et al. (2017), 3D stresses/strains are found to be important in the failure of a 52.3m blade and solid elements are recommended in FE simulation when the failure is of concern. Please comment on the shell elements used in this study and maybe state the scope of this study in the introduction.

Response to Comment 4:

The scope of our investigation is limited to the finite element investigation of the strength of an existing 5m blade in terms of composite material failure.

Following the suggestion of the Referee, the following paragraph will be included in the introduction of the manuscript:

"Chen, Zhao and Xu (2017) (https://doi.org/10.1002/we.2087) found 3D stresses/strains to be important in the failure of a 52.3-meter blade and solid elements recommended in the FE simulation when debonding failure is of concern. They utilized 3-D strains and Yeh-Stratton failure criterion to calculate delamination and debonding failures in the blade. The scope of this work is limited to the investigation of the structural response of a 5-meter blade using global Finite Element Modeling approach and progressive composite failure analysis. For this structural analysis global FE Model is meshed using plane stress shell elements. Using the current modeling technique with shell elements critical locations for failure and worst load case scenario are identified. Puck's 2-D damage model demonstrates the direction to proceed for a complete and comprehensive modeling of the failure mechanisms. Furthermore, within the framework of this study, differences between edgewise, flap-wise and combined flap-wise/edgewise loading conditions are discussed."

Comment 5: In Fig. 4, it seems that the stress-strain curves are rather linear. How can one see that the nonlinear Puck material damage model used in this study is superior to other models, even to the linear ones?

Response to Comment 5:

Following the comment of the Referee, we notice that we misused terms in our paper that led to confusion and misunderstanding. We made changes to the terminology. We changed the term "linear model (Puck)" to the correct term "linear elastic model" and "nonlinear model (Puck progressive)" to "progressive damage model". This is more appropriate since in the "linear model (Puck)", only linear elastic model is used and no damage is implemented. In the "nonlinear model", progressive damage algorithm is used. The text will be corrected with correct terminology in the revised manuscript. As stated in the methodology section of the manuscript, Puck's progressive damage model (Puck and Schuermann, 1998) (https://doi.org/10.1016/S0266-3538(96)00140-6) is implemented in the ANSYS. Puck's model (Puck and Mannigel, 2007) (https://doi.org/10.1016/j.compscitech.2006.10.008) which incorporates "non-linear stress-strain relations for the inter-fibre fracture analysis of FRP laminates" is not used in this study.

Regarding our decision for the damage model used in our study, we would like to point out that all failure criteria have advantages and disadvantages. We decided to use Puck's progressive damage model because Puck's theory is based on fracture planes and Mohr-Coulomb's hypothesis and enables differentiation between fiber and three different inter-fiber failure modes (IFF(A), IFF(B) and IFF(C)). We have chosen to implement Puck's failure model to have a more detailed understanding of the failure modes. In the past, the authors have compared Puck's and Tsai-Wu failure models, albeit nonprogressive implementation, for the strength analysis of a 5-m wind turbine blade and found that Tsai-Wu (1971) delivers more conservative results compared to Puck (Ozyildiz, Muyan, Coker, IOP TORQUE 2018) (https://doi.org/10.1088/1742-6596/1037/4/042027).

Comparison of Puck with Tsai-Wu and other failure criteria was not studied in the manuscript because it was not in the scope of this study. However, comparison was made in the literature, namely World Wide Failure Exercise (WWFE) I Part B (Hinton et al, 2002) (https://doi.org/10.1016/S0266-3538(02)00125-2)for the original Tsai- Wu (1971) (https://doi.org/10.1177%2F002199837100500106) which did not perform as well as Puck (1998). As an example, comparison between the predicted and measured biaxial failure envelopes for [0/±45/90]s CFRP/AS4 3501-6 laminates shown in Figure R 1 demonstrates that in the third quadrant under compression-compression stresses Tsai (1971)'s prediction becomes quite non-conservative compared to the prediction of other failure theories. Moreover, the original Tsai-Wu (1971) is not capable of differentiation between different failure modes whereas DNV GL Standard (2015) (https://rules.dnvgl.com/docs/pdf/DNVGL/ST/2015-12/DNVGL-ST-0376.pdf) requires a separate strength verification for fiber and inter-fiber failure modes such as Puck or LARC03.

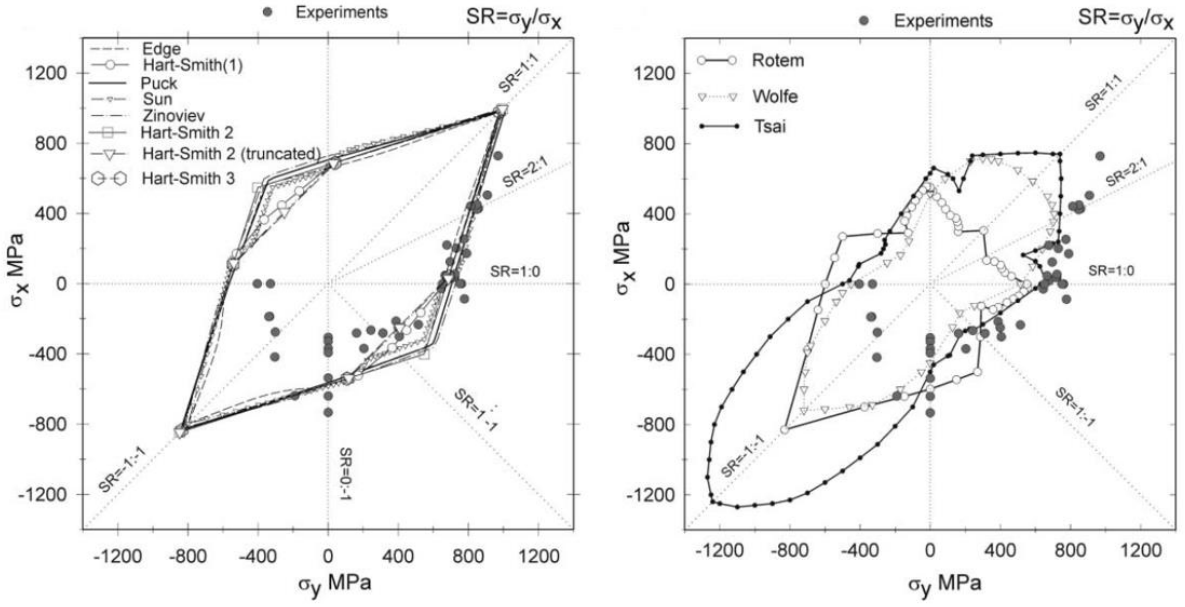

(a) (b)

Figure R 1. (a) and (b) Comparison between the predicted and measured biaxial failure envelopes for [0/±45/90]s CFRP/AS4 3501-6 laminates (Hinton et al., 2002) (https://doi.org/10.1016/S0266-3538(02)00125-2).

Comment 6: In Fig. 4, please also show the comparison when the other models are used, e.g., the normal Puck, Tsai-Wu, etc.

Response to Comment 6:

As mentioned in answer 5, we changed the misleading terminology from linear model (Puck) to linear elastic model and nonlinear to progressive damage model. The text will be corrected with correct terminology in the revised manuscript.

The comparison recommended by the Referee has been carried out in the literature. Figure R 1 shows Fig. 4 as taken from the World Wide Failure Exercise (WWFE) I Part B (Hinton et al, 2002) that compares the stress-strain curves for [0/90]s GFRP and [0/±45/90]s CFRP laminates. As seen from Figure R 2, Tsai-Wu (1971) underpredicted the laminate strength for GFRP/MY750 and CFRP/AS4 3501-6 laminates under uniaxial tension. If the Referee recommends the comparison of the modified version of the original Tsai-Wu (1971) model as explained in Chen, Wei Zhao, Lu Zhao and Xu (2014) in which failure mode-based material degradation is used, it can be implemented in the revised manuscript.

We would like to emphasize that these comparisons are for the original Tsai-Wu (1971) while the modified version in the study (Liu and Tsai, 1998) (https://doi.org/10.1016/S0266-3538(96)00141-8) has been shown to be more accurate as stated in the conclusions: "the Tsai theory proved to be in the leading group of those tested in the 'exercise'."

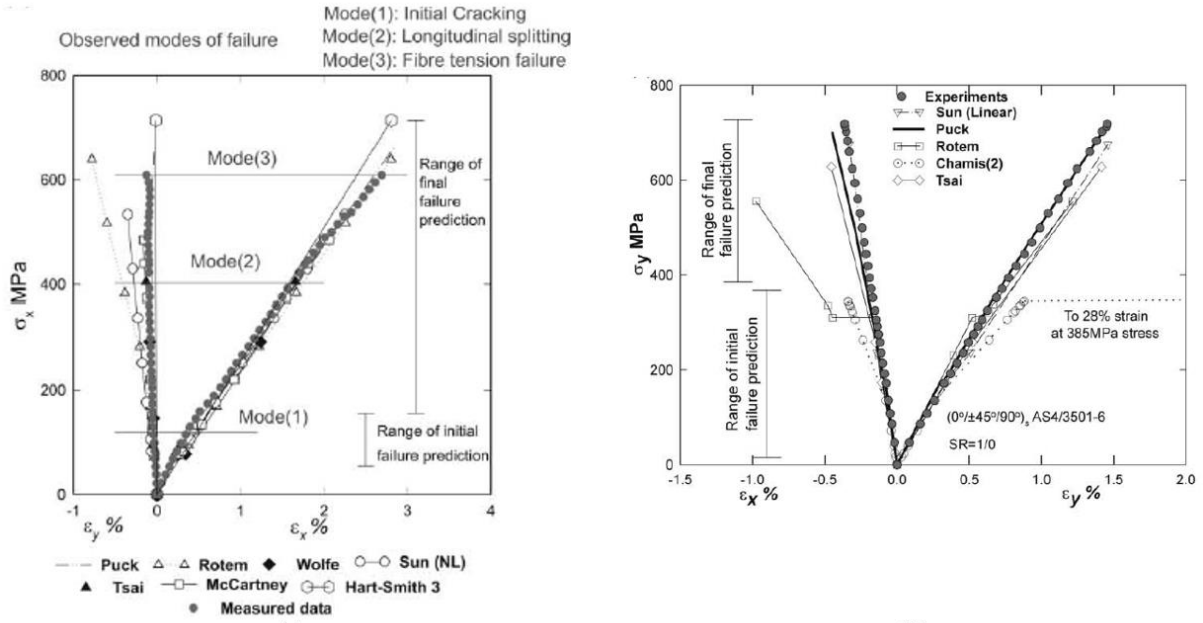

Figure R 2. (a) Comparison between measured and predicted stress-strain curves for [0/90]s GFRP/MY750 laminate under uniaxial tension $\boldsymbol{\sigma_y = 0}$ (b) Comparison between measured and predicted stress-strain curves for [0/±45/90]s CFRP/AS4 3501-6 laminate under uniaxial tension $\boldsymbol{\sigma_x = 0}$ (Hinton et al., 2002) (https://doi.org/10.1016/S0266-3538(02)00125-2).

Comment 7: In Fig. 10 and the other similar figures, please compare when the other models are used, e.g., the normal Puck, Tsai-Wu, etc. Modern FE software provide the built-in composite damage models for shell elements, please include the comparison in relevant curves.

Response to Comment 7:
As mentioned in response 5, we changed the terminology linear model (Puck) to linear elastic model and nonlinear model (progressive Puck) to progressive damage model. The text will be corrected with correct terminology in the revised manuscript.

We are using ANSYS Version 17.2 for our FE Simulations and only the original version of Tsai-Wu (1971) model is available as the built-in Tsai-Wu composite damage model in ANSYS. Since Tsai-Wu (1971) did not perform as well as Puck (1998) failure criteria as detailed in our response to comments 5 and 6, we did not compare Puck with Tsai-Wu. If recommended by the Referee, a new ANSYS APDL script can be written in order implement the modified Tsai-Wu model explained in Chen, Wei Zhao, Lu Zhao and Xu (2014). Afterwards, the comparison can be done. However, we believe comparison of advanced failure models is outside the framework of this paper.

Comment 8: In Fig. 12 (d), why there is considerable damage at the blade tip, which is usually not loaded.

Response to Comment 8:

We like to thank the referee for this observation, and as a result we conducted a detailed investigation for the damage at the blade tip. We noticed unmerged nodes at the suction side tip and created a new finer mesh as seen in Figure R 3 below. In addition to the merging nodes at the tip of the suction side, the overall mesh structure of the blade is improved. In the updated FE Model of the blade there are 63104 elements. After running the updated FE Model Fig. 10 (Figure R 4) and Fig. 12(Figure R 5) in the manuscript are updated as seen below.

Element failure progression in the pressure side, internal flange and suction side of the blade is depicted in Figure R 5 below. According to the analysis results, element failure is observed in the internal flange at 90% loading. As seen from Figure R 5 failure in the internal flange grows further as the load is increased to 100%. At 160% loading in addition to the damaged region in the internal flange, damage grows along the trailing edge, pressure side and leading edge. Shortly before collapse at 180% loading, damaged regions at the leading and trailing edges evolve further and damage at the blade tip occurs. The reasons for damage initiation at the blade tip at the most extreme load level can be explained as follows:

- From Figure 7 in the manuscript it is seen that there is although low, some loading on the blade tip. At 180%, 1.8 times the extreme flap-wise loading, which read is from Figure 7 is applied to the blade and the blade collapses afterwards.

- Blade tip structure is rather thin and less stiff compared to other regions of the blade.

- As seen in Figure R 5(d) at 180% load level trailing edge and the internal flange which is used to bond the pressure and suction sides of the blade are already damaged. As a consequence, towards the blade tip the pressure and suction sides of the blade are detached at this load level. Under these circumstances blade tip structure is weaker and can be damaged more easily.

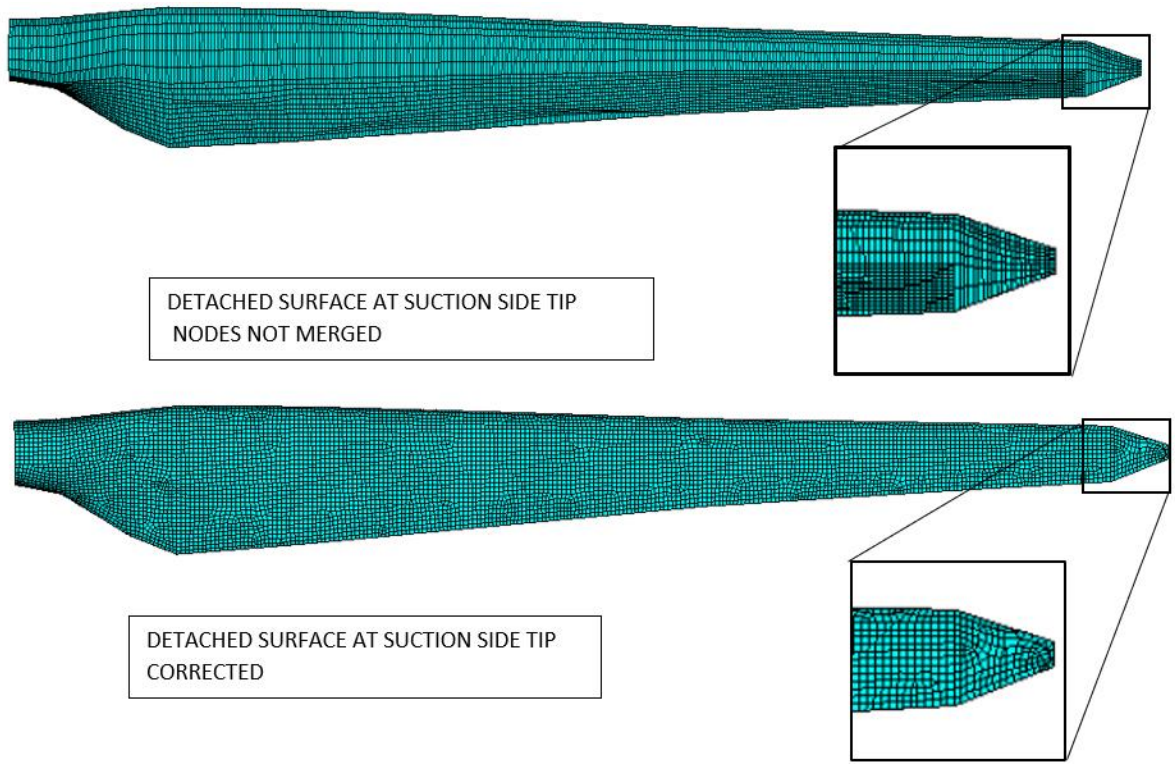

Figure R 3. Correction of the unmerged nodes at the blade suction side tip.

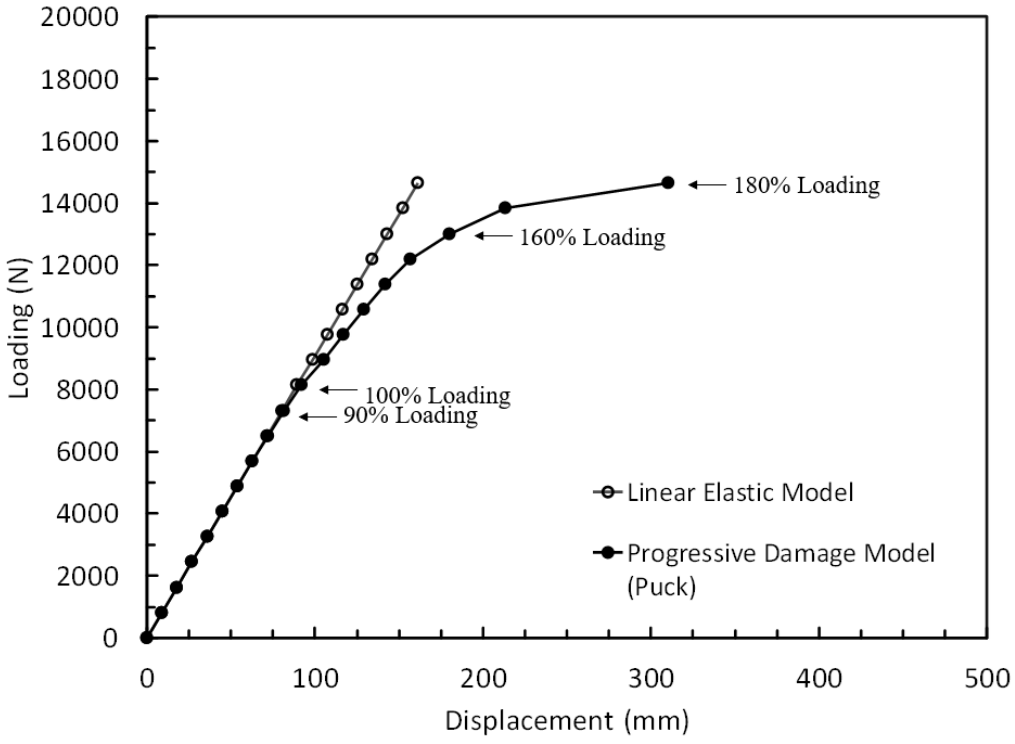

Figure R 4. Load displacement curves of the blade using the linear elastic model and progressive damage model (Puck) under extreme flap-wise loading. (This figure updates Figure 10 in the original manuscript).

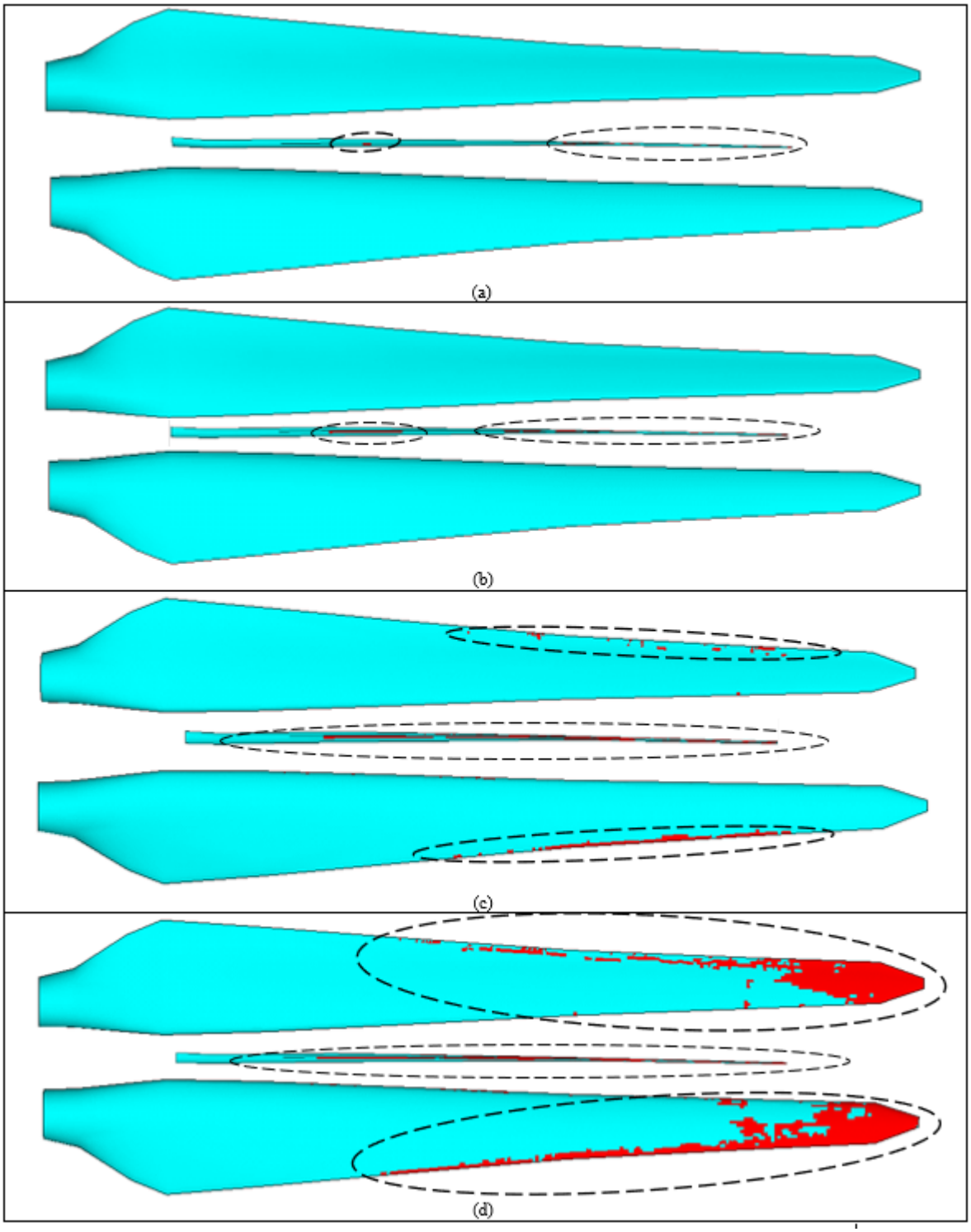

Figure R 5. Element failure progression in the pressure side, internal flange and suction side of the blade (from top to bottom in a row) at (a) 90%, (b) 100%, (c) 160% and (d) %180 of extreme flap-wise loading. (This figure updates Figure 12 in the original manuscript).

Comment 9: in Fig. 15(d), why there is an undamaged region (blue) enclosed by the damaged region (red)?

Response to Comment 9:

After running the updated FE Model (See response 8) Fig. 15 (Figure R 6) in the manuscript are updated as seen below.

Damage progression regarding inter-fiber-failure (IFF) C and Fiber-failure (FF) in detail section D of the blade is investigated in Figure R 6. IFF (C) and FF stress exposures (Puck's terminology for failure index) are shown on the same plot. If both IFF (C) and FF failures are present in an element the greater stress exposure FF or IFF (C) is depicted.

In Figure R 6 (d) dark blue regions enclosed by the damaged region (red) are the 'killed' elements from previous load steps. At the end of a load step, if the stress exposure FF or IFF(C) exceeds one (red regions), the elements are deactivated by the EKILL command in ANSYS. A deactivated element remains in the model but contributes an almost zero value to the overall stiffness matrix. Dark blue represents 'zero' stress exposure, because there exists no stress in these 'killed' elements. The new damaged region in red evolves around the 'killed' elements. The new damaged region in red together with dark blue region form the new group of 'killed' elements. This new group of 'killed' elements are the failed elements depicted in red in Figure R 5 (d).

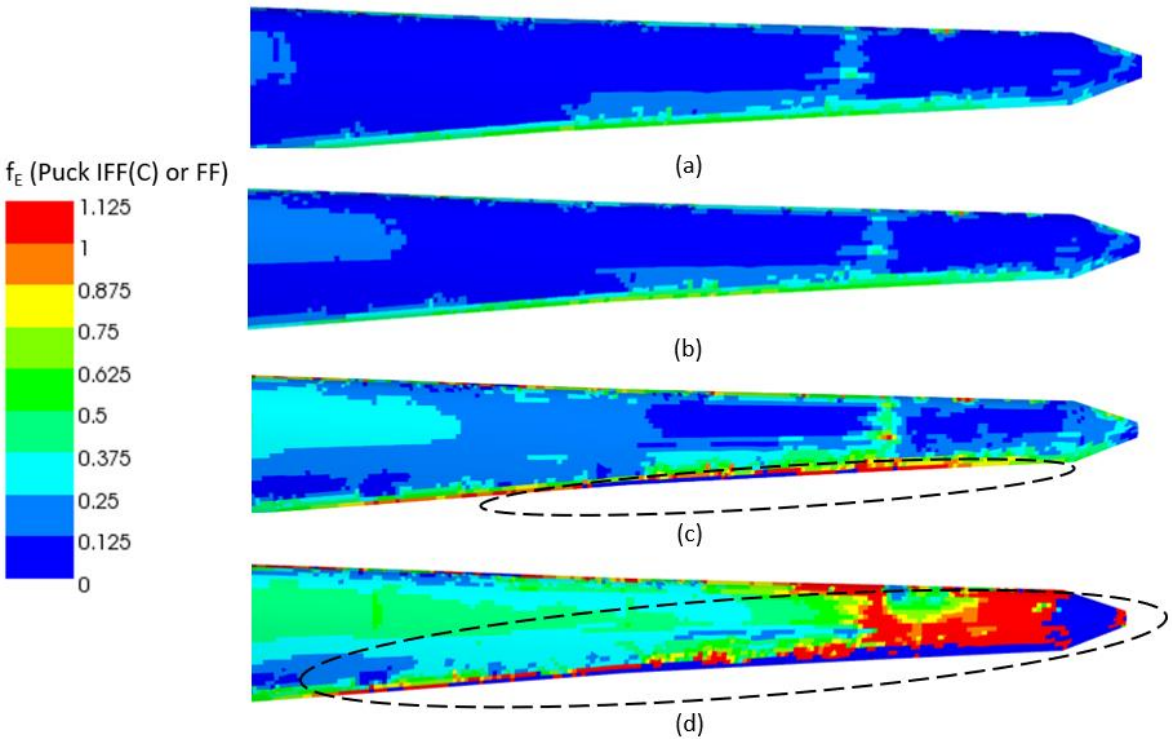

Figure R 6. Failure progression on the blade suction side at (a) 90%, (b) 100%, (c) 160%, and (d) %180 of extreme flap-wise loading in detail D. (This figure updates Figure 15 in the original manuscript).

Comment 10: In Fig. 16 and other similar figures, please also show what is happening in the blade model at the turning points, is it due to local or global buckling?

Response to Comment 10:

A linear buckling analysis of the blade is performed in order to investigate its buckling resistance and location of buckling eigenmodes. The results are depicted in Figure R 7. Negative eigenvalues correspond to the loads applied in the opposite direction, because no critical eigenvalue could be found in the load application direction. In other words, the blade exhibits sufficient buckling resistance for edgewise and combined edgewise and flap-wise loading. According to GL 2010 the load factor should be greater than 1.25, which is fulfilled for all the load cases studied. We observe that the eigenmodes are located in the sharp trailing edge structure for edgewise and combined edgewise and flap-wise loading cases. For the extreme flap-wise load case, eigenmode location is towards blade tip.

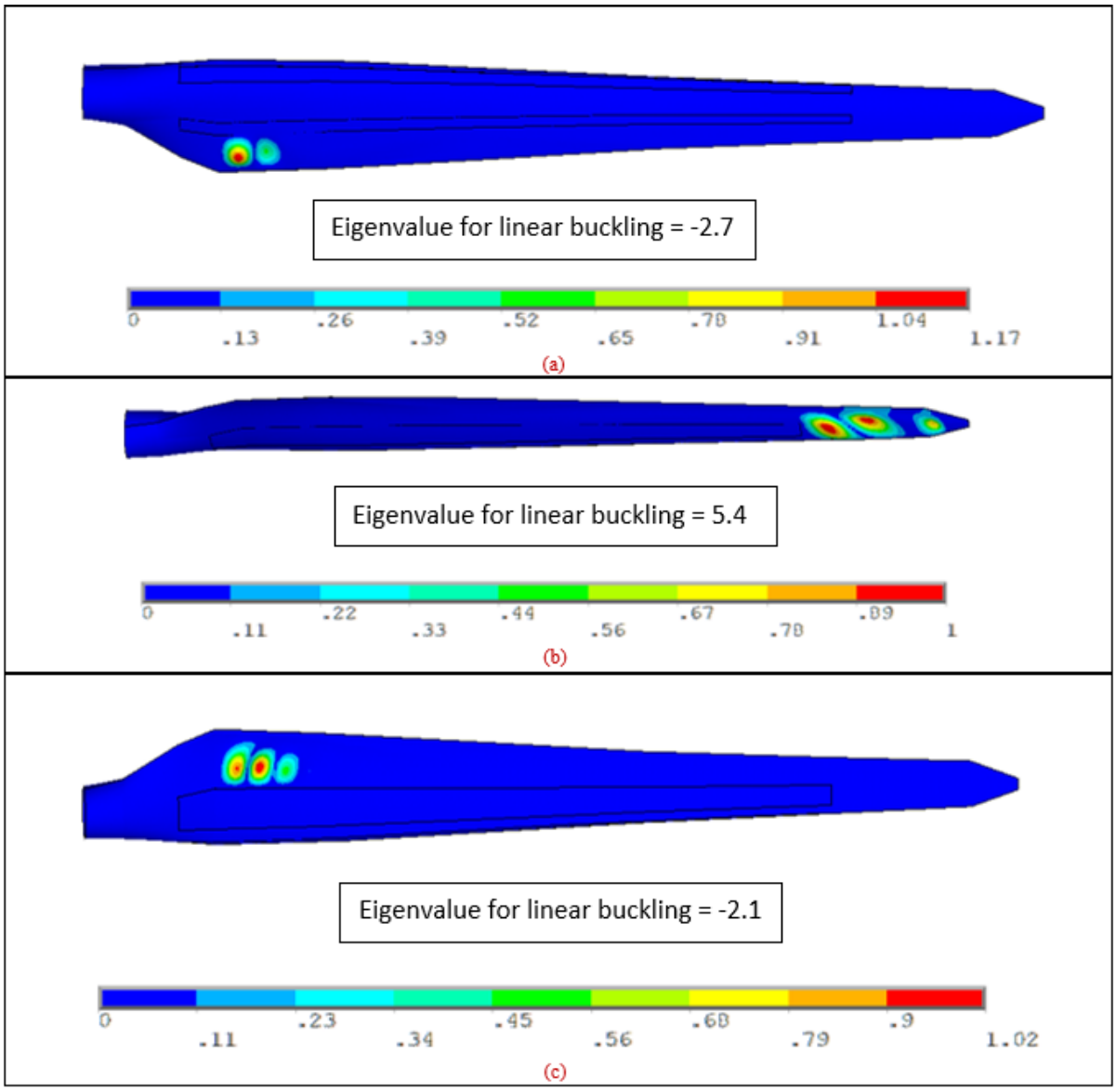

Figure R 7. Buckling modes of the blade under (a) 100% edgewise(min) loading case (b) 100% flap-wise(max) loading case (c) 100% combined edgewise(min) and flap-wise(max) loading. (Color bar shows total deformation).

According to Chen, Zhao und Xu (2017) a linear buckling analysis always predicts the upper borderline for the buckling factor, for a more realistic buckling analysis a nonlinear buckling analysis including geometric and material nonlinearity (degradation) is necessary.

After improving the mesh structure of the blade Fig. 24 (Figure R 8) is updated as seen below (See response to comment 8). In Figure R 8, turning points are marked for different load cases.

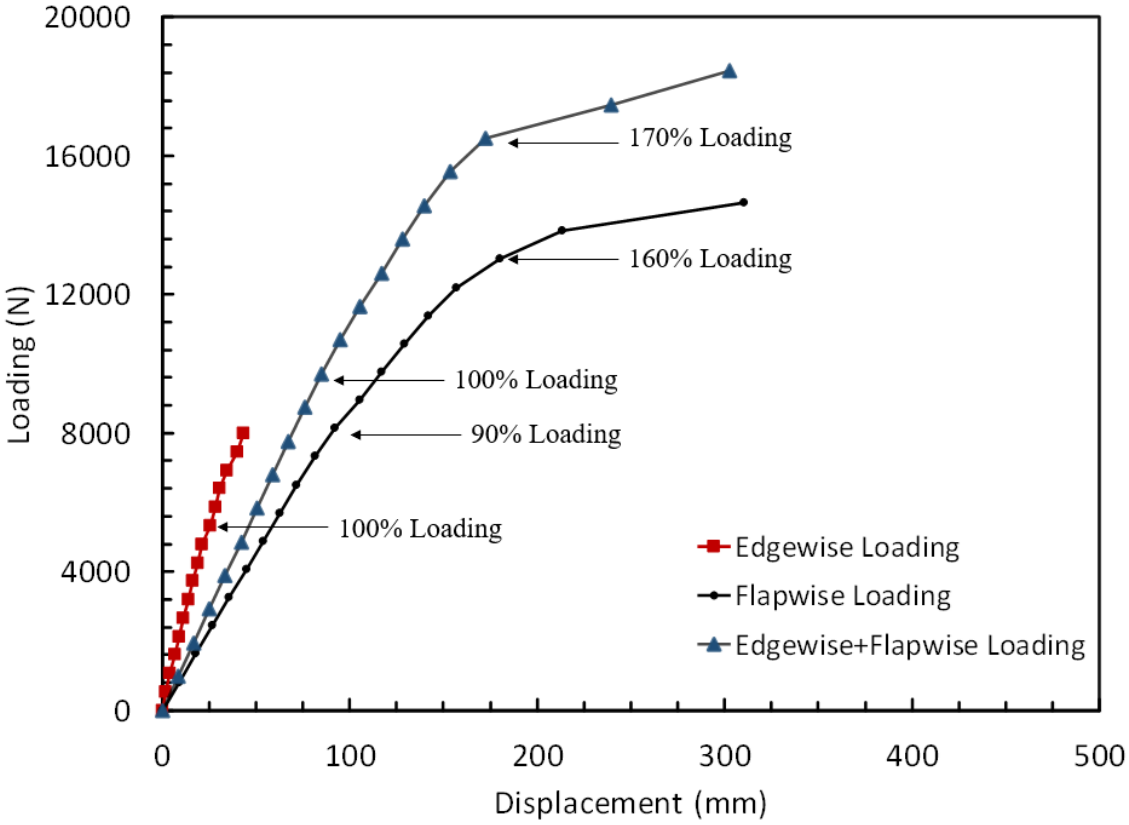

Figure R 8. Load displacement curves of the blade under edgewise, flap-wise, and edgewise plus flap-wise loading. (This figure updates Figure 24 in the original manuscript).

In Figure R 8 at the turning point which corresponds to 100% edgewise loading, the stiffness of the failed elements in suction side towards blade root are set to zero and total deformation due element failure in this area is observed as depicted Figure R 9 below.

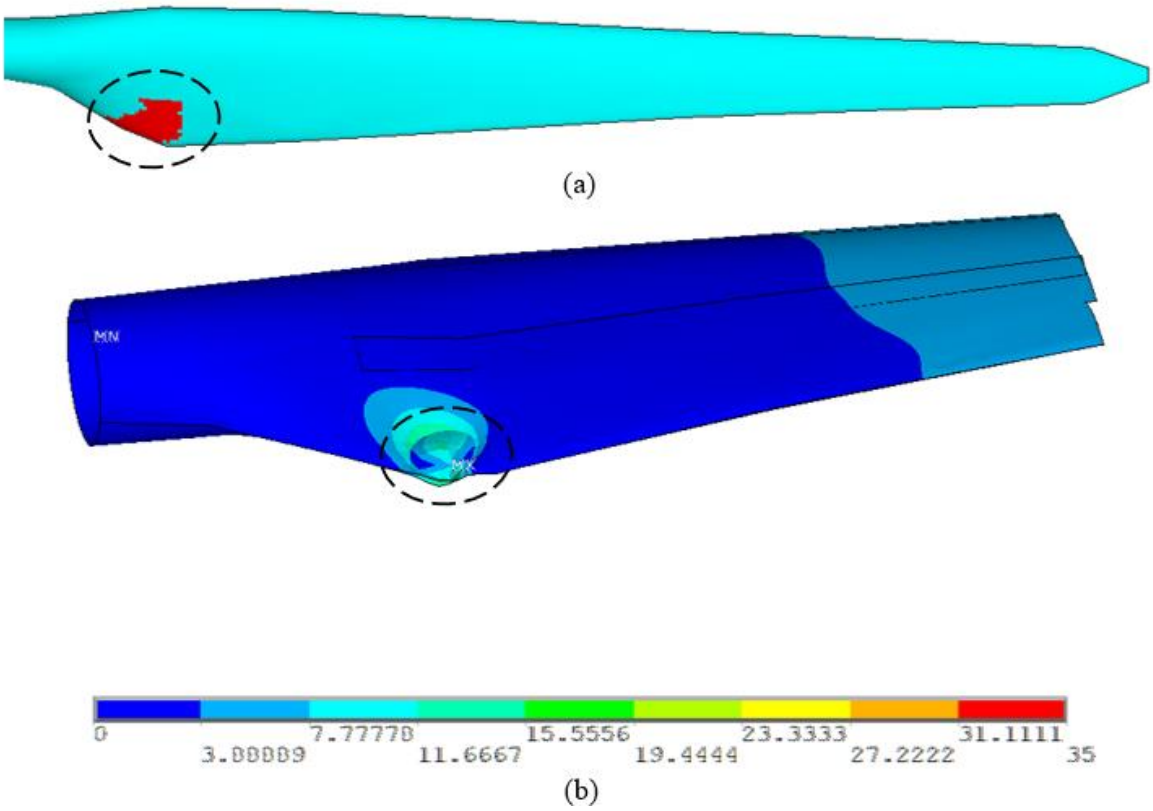

Figure R 9. Failure evolution in the suction side of the blade at 100% edgewise loading (a) failed (killed) elements (b) total deformation due to failed elements.

For flapwise loading, first slight turning point due to the failure of elements in the internal flange is observed at 90% flap-wise load. At this load level, damage in the internal flange is shown in Figure R 5 (a). Second more obvious turning point is observed at 160% flap-wise loading. At this load level Figure R 5 (c) shows laminate failure in the internal flange and trailing edges. Due to element failure, deformation in the form of local buckling at the trailing edge is observed as depicted in Figure R 10 below.

For combined flap-wise and edgewise loading, similarly, first slight turning point due to the failure of elements in the internal flange is observed at 100% of combined loading. Damage in the internal flange is shown in Figure R 11 (a). Second more obvious turning point is observed under 170% combined flap-wise and edgewise loading. At this load level Figure R 11 (b) shows laminate failure in the internal flange, trailing edge and blade tip. Due to element failure, deformation in the form of local buckling at the trailing edge is observed as depicted in Figure R 11 below.

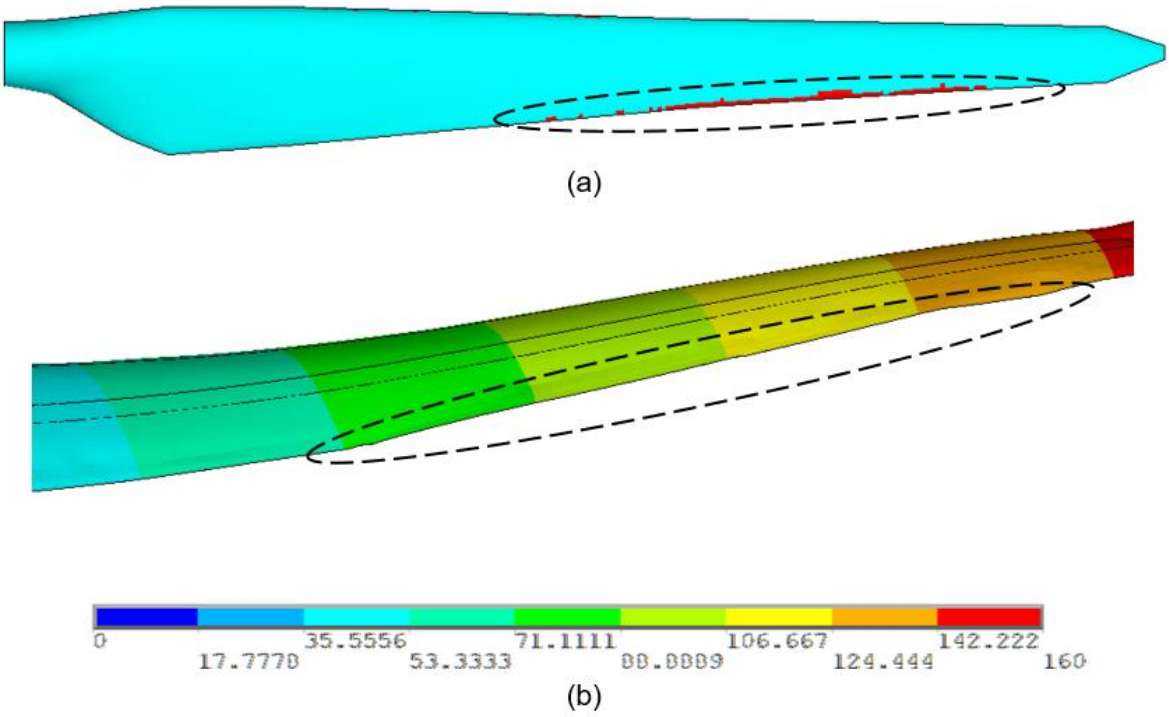

Figure R 10. Failure evolution in the trailing edge of the blade at 160% flap-wise loading (a) failed (killed) elements (b) total deformation occurring in form of local buckling due to failed elements.

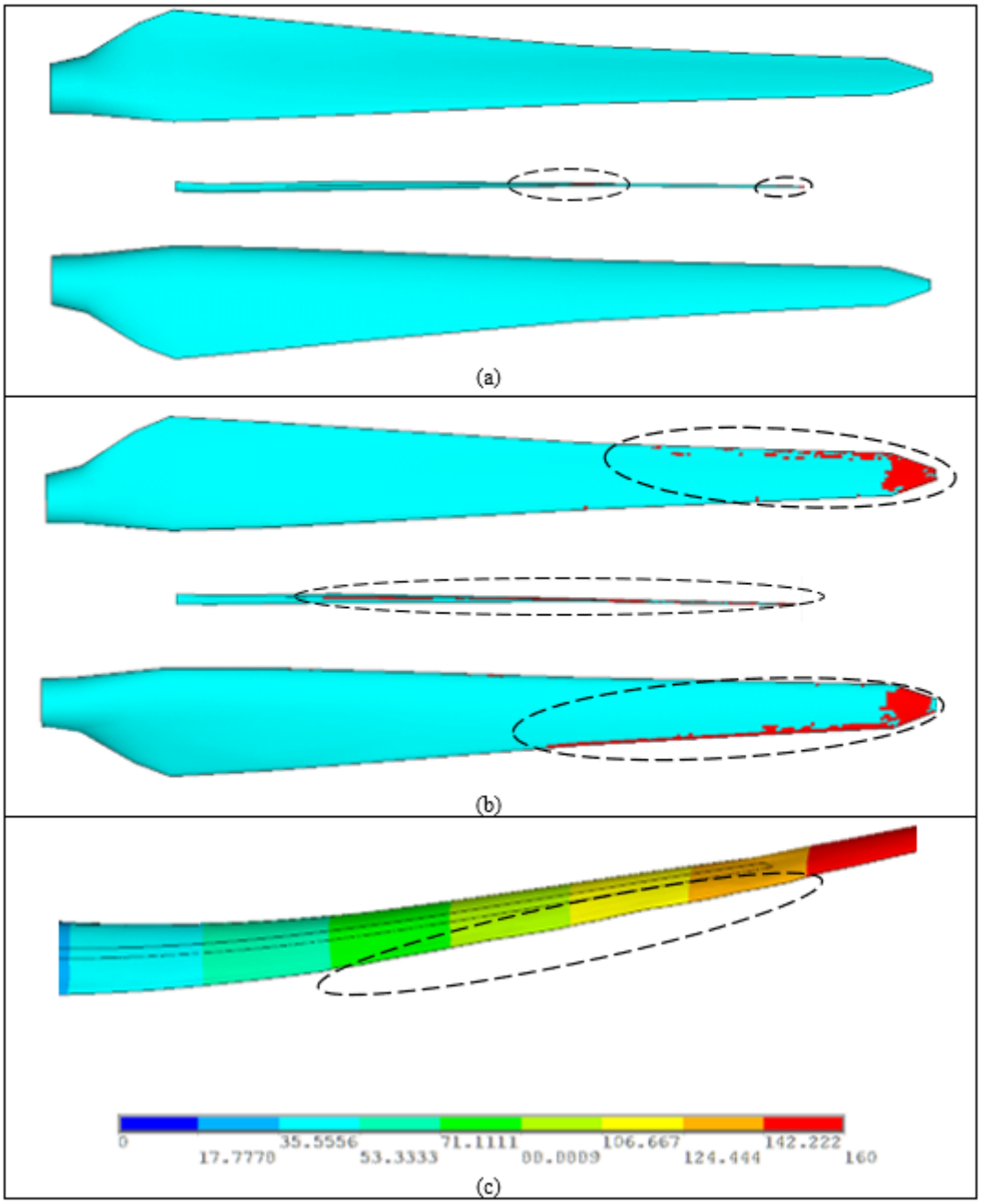

Figure R 11. Failure evolution in the pressure side, internal flange and suction side of the blade (from top to bottom in a row) at (a) 100% (b) 170 % combined edgewise and flap-wise loading (c) total deformation occurring in form of local buckling due to failed elements at 170 % combined edgewise and flap-wise loading.

Comment 11: In Fig. 19(c) and 19(d), why do the damaged regions heal? It is better to show the damage status rather than the Puck index. Like the one used in https://doi.org/10.3390/en7042274

Response to Comment 11:

After improving the mesh structure of the blade Fig. 16 (Figure R **12**) and Fig 19 (Figure R **13**) are updated as seen below (See response 8).

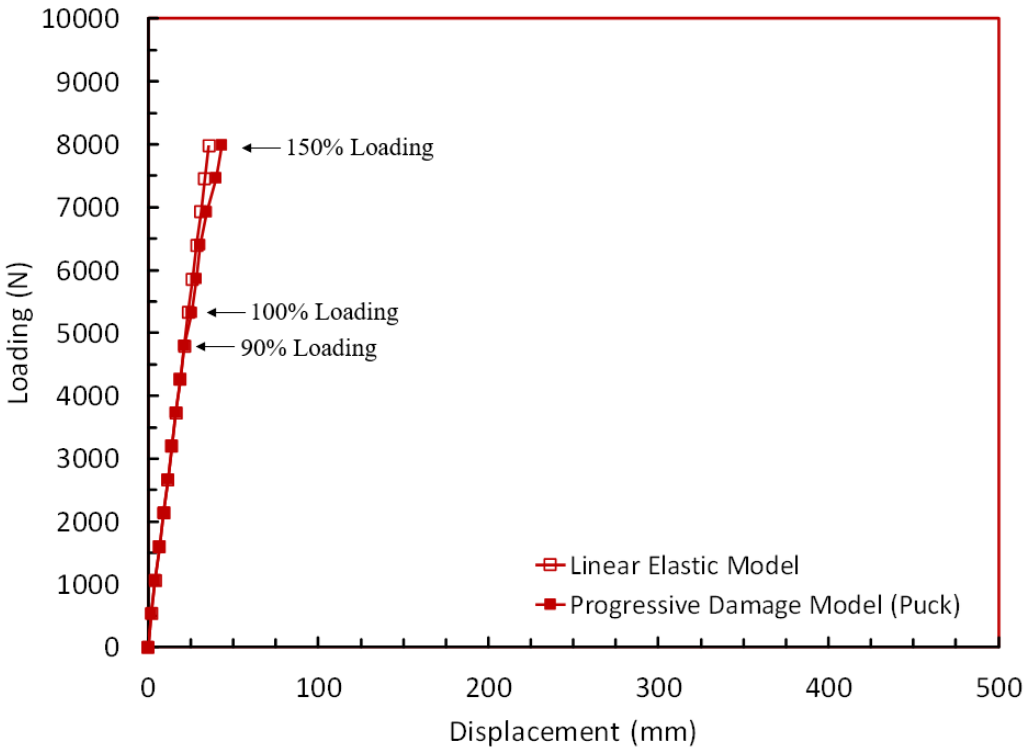

Figure R 12. Load displacement curves of the blade using the linear elastic model and Puck progressive model under edgewise loading. (This figure updates Figure 16 in the original manuscript).

In Fig. 19(c) and Fig 19(d) the dark blue regions inside red(damaged) regions do not mean that the damaged regions heal. Dark blue regions correspond to the 'killed' (failed) elements from previous load steps. Since the stiffness of the 'killed' elements are set to zero, they show no stress under loading. Hence their stress exposure (Puck's terminology for failure index) is calculated as zero and they appear as dark blue regions under red regions. For a more detailed explanation to this question please refer to the response of comment 9.

As recommended by the Referee the illustration of the damaged status is changed as depicted in Figure R 13 below:

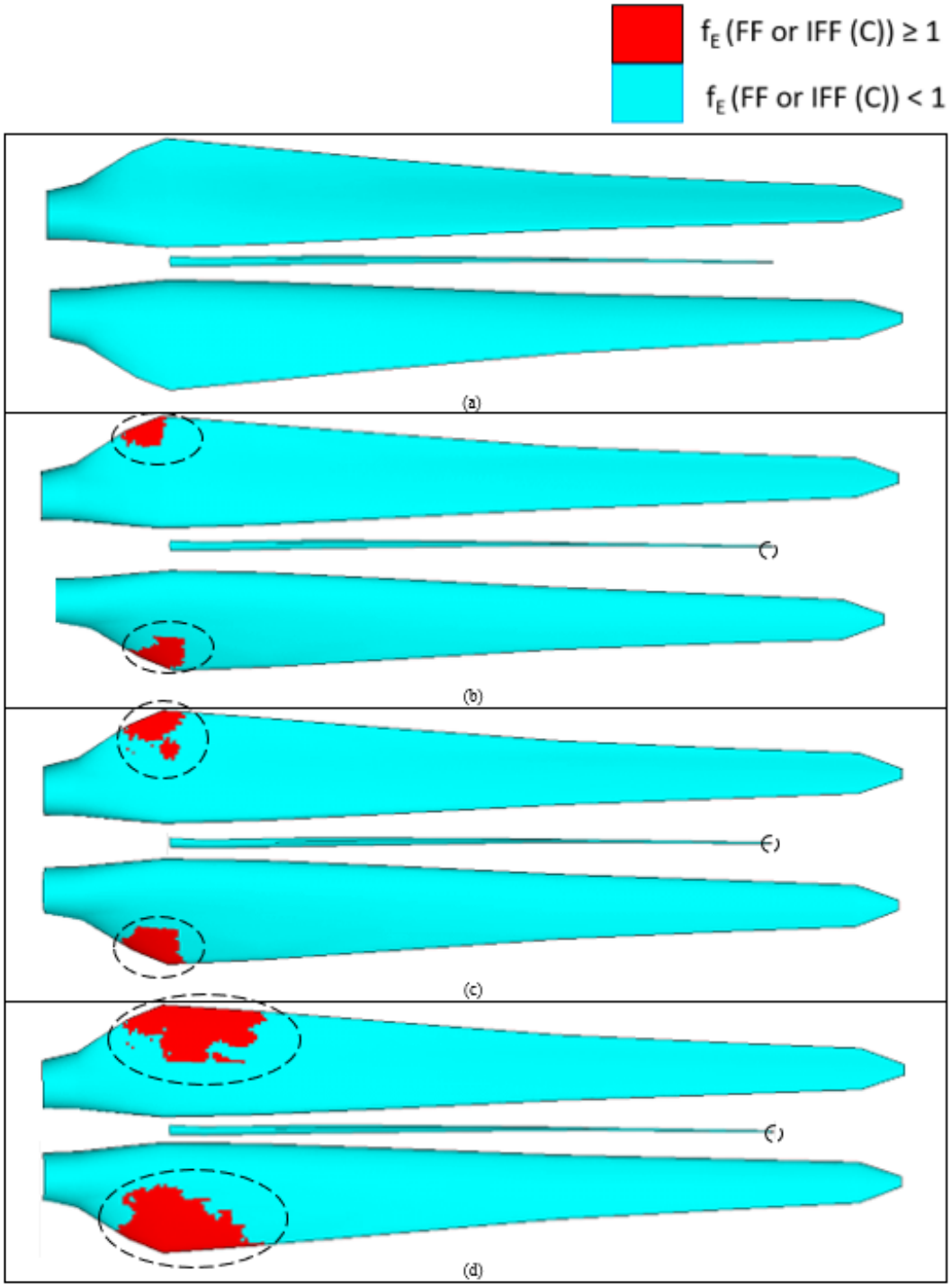

Figure R 13. Failure progression on the blade pressure side, internal flange and suction side (from top to bottom in a row) at (a) 90%, (b) 100%, (c) 120% and (d) 150% of extreme edge-wise loading. (This figure updates Figure 19 in the original manuscript).